Characterization of the enzymatic activity of Clostridium perfringens TpeL

Serge Pauillac, Jacques d'Allayer, Pascal Lenormand, Jean Claude Rousselle, Philippe Bouvet, Michel Popoff

Elsevier Editorial System(tm) for Toxicon
Manuscript Draft

Manuscript Number:

Title: CHARACTERIZATION OF THE ENZYMATIC ACTIVITY OF Clostridium perfringens TpeL

Article Type: From Threats to Benefits

Keywords: Clostridium perfringens, toxin, TpeL, GTPase, Ras, Rho, Rac glucosylation

Corresponding Author: Dr Michel Popoff, Dr

Corresponding Author's Institution: Institut Pasteur

First Author: Serge Pauillac

Order of Authors: Serge Pauillac; Jacques D'Alayer; Pascal Lenormand; Philippe Bouvet; Michel Popoff, Dr

Abstract: TpeL is a toxin produced by Clostridium perfringens which belongs to the large clostridial glucosylating toxin family. It was shown that TpeL modifies Ras using UDP-glucose or UDP-N-acetylglucosamine as cosubstrates (Guttenberg et al., 2012; Nagahama et al., 2011). We confirmed that TpeL preferentially glucosaminates the three isoforms of Ras (cH-Ras, N-Ras, and K-Ras) from UDP-N-acetylglucosamine and to a lower extent Rap1a and R-Ras3. In contrast to previous reports, we observed that Rac and Ral are no substrates of TpeL. In addition, we confirmed by in vitro glucosylation and mass specgtrometry that TpeL modifies cH-Ras at Thr35.

Suggested Reviewers: Ralf Gerhard
Gerhard.ralf@mh-hannover.de
Expert in clostridium toxins

Gilles Prevost
prevost@unistra.fr
Expert on bacterial toxins

Francisco Uzal
fuzal@cahfs.ucdavis.edu
Expert in Clostridium perfringens

Opposed Reviewers: Klaus Aktories
Conflict of interest

Highlights

- TpeL is a cytotoxin produced by *Clostridium perfringens* which belongs to the large clostridial glucosylating toxin family

- TpeL uses both UDP-glucose and UDP-*N*-acetylglucosamine as cosubstrates but preferentially this latter.

- TpeL modifies mainly cH-Ras, N-Ras, K-Ras and to a lower extent Rap1a, R-Ras3, and Rac1

- TpeL modifies cH-Ras at Thr35

CHARACTERIZATION OF THE ENZYMATIC ACTIVITY OF *Clostridium perfringens* TpeL

Serge PAUILLAC[1], Jacques D'ALLAYER[2], Pascal LENORMAND[2], Jean Claude ROUSSELLE [2], Philippe BOUVET[1], Michel R. POPOFF[1]

[1]Institut Pasteur, Unité des Bactéries anaérobies et Toxines, 75724 Paris cedex15, France

[2]Institut Pasteur, Plateforme Protéomique, 75724 Paris cedex15, France

Running title: *Clostridium perfringens* TpeL

Key words: *Clostridium perfringens*, toxin, TpeL, GTPase, Ras, Rho, Rac glucosylation

Correspondence to Michel R. Popoff, Institut Pasteur, Unité des Bactéries anaérobies et Toxines, 25 rue du Dr Roux, 75724 Paris cedex 15, France

Tel: 33 1 45688307

Fax: 33 1 45613123

mpopoff@pasteur.fr

Abstract

TpeL is a toxin produced by *Clostridium perfringens* which belongs to the large clostridial glucosylating toxin family. It was shown that TpeL modifies Ras using UDP-glucose or UDP-*N*-acetylglucosamine as cosubstrates (Guttenberg *et al.*, 2012; Nagahama *et al.*, 2011). We confirmed that TpeL preferentially glucosaminates the three isoforms of Ras (cH-Ras, N-Ras, and K-Ras) from UDP-*N*-acetylglucosamine and to a lower extent Rap1a and R-Ras3, and very weakly Rac1. In contrast to previous report, we observed that Ral was not substrate of TpeL. In addition, we confirmed by *in vitro* glucosylation and mass spectrometry that TpeL modifies cH-Ras at Thr35.

1. Introduction

Clostridium perfringens is an ubiquitous anaerobic bacterium which is responsible for mild to severe diseases in humans (gas gangrene, gastrointestinal diseases) and animals (mainly gastrointestinal and enterotoxemic diseases). The pathogenicity of this microorganism is based on protein toxins, which are secreted in the culture medium, gastrointestinal tract or tissues (Popoff and Bouvet, 2009). *C. perfringens* is among the bacteria which produce the greatest number of toxins. According to the toxins, which are synthesized, *C. perfringens* strains are divided into several toxinotypes (Petit *et al.*, 1999). Recently, a new toxin, called TpeL (for toxin *C. perfringens* large cytotoxin), was identified in several strains of *C. perfringens* type B and C. TpeL was found to be lethal for mice and cytotoxic for Vero cells and shows a significant homology of its N-terminal region with the catalytic domain of the large glucosylating clostridial toxins which encompass *Clostridium difficile* toxin A (TcdA) and toxin B (TcdB), *Clostridium sordellii* lethal toxin (TcsL) and hemorrhagic toxin (TcsH), and *Clostridium novyi* alpha toxin (TcnA) (Amimoto *et al.*, 2007).

Large glucosylating clostridial toxins (LGCTs) contain at least three functional domains. The one third C-terminal part exhibits multiple repeated sequences (31 short repeats and 7 long repeats in TcdA), which are involved in the recognition of a cell surface receptor. The central part contains a hydrophobic segment and probably mediates the translocation of the toxin across the membrane. The enzymatic site characterized by the DxD motif surrounded by a hydrophobic region, and the substrate recognition domain are localized within the 543 N-terminal residues corresponding to the natural cleavage site in TcdB (Hofmann *et al.*, 1998; Hofmann *et al.*, 1997; Rupnik *et al.*, 2005). The overall structure of the enzymatic domains of TcdB, TcsL and TcnA is conserved and consists of a β-strain

central core (about 235 amino acids) forming an active center pocket surrounded by numerous α-helices (Jank and Aktories, 2008; Reinert *et al.*, 2005; Ziegler *et al.*, 2008). LGCTs catalyze the glucosylation of Rho- and/or Ras-GTPases from UDP-glucose, except TcnA, which uses UDP-*N*-acetylglucosamine as cosubstrate. The glucosylating activity supports the main biological activities of these toxins. But, LGCTs differ in their substrates. Thereby, TcdA and TcdB glucosylate Rho, Rac and Cdc42 at Thr-37, whereas LcsT glucosylates Ras at Thr-35, Rap, Ral and Rac at Thr-37 (Just and Gerhard, 2004; Popoff and Bouvet, 2009). The structural basis of the different recognition of substrates is not well known. Differences in α-helices, insertions-deletions, probably account for the substrate specificity of each toxin (Reinert et al., 2005; Ziegler et al., 2008). Chimeric molecules between TcdB and TcsL have been used to identify the sites of Rho-GTPase recognition. Amino acids 408 to 468 of TcdB ensure the specificity for Rho, Rac and Cdc42, whereas in TcsL, the recognition of Rac and Cdc42 is mediated by residues 364 to 408, and that of Ras proteins by residues 408 to 516 (Hofmann et al., 1998; Jank *et al.*, 2007). Since TpeL seems to be a natural variant of large glucosylating clostridial toxins, the characterization of its enzymatic activity and substrate specificity would permit to better understand the structure/function of this group of toxins.

In this study, we show that TpeL is a glucosylating toxin which targets Ras proteins and to a lower extent Rap and R-Ras3, and preferentially uses UDP-*N*-acetylglucosamine as cosubstrate. Similarly to *C. sordellii* TcsL, TpeL monoglucosylates Ras at Thr35. During the progress of this work, related results have been published (Guttenberg et al., 2012).

2. Materials and methods

2.1 Reagents

Uridine-5-diphospho(UDP)-glucose, UDP-*N*-acetylglucosamine, UDP-galactose, UDP-glucuronic acid, UDP-galacturonic acid, UDP-mannose, ADP-glucose, ADP-ribose, CDP-glucose, GDP-glucose, TDP-glucose were from Sigma. Plasmids encoding Rho-, Rac-, Cdc42-GST proteins were from A. Hall.

2.2 Production and purification of recombinant TpeL N-terminus (rN-TpeL)

The DNA coding for the N-terminal part of TpeL was PCR amplified from *C. perfringens* type B strain NCTC3181 with primers adding a *Bam*HI site at the 5' end and a *Sal*I site at the 3' end. The PCR product was cloned into pCR2.1 vector (Invitrogen), and the digested insert with *Bam*HI-*Sal*I was subcloned into pET28a (Novagen) at the corresponding sites. The recombinant protein was fused to an N-terminal extension containing a 6-histidine

motif from pET28.

E. coli BL21 CodonPlus (DE3)-RIL (Stratagene) transformed with recombinant plasmids respectively were grown in LB medium containing kanamycine (50 μg/ml) at 26° C until a OD of 0.8. The expression was induced with IPTG (1 mM) and growth was continued overnight at 26° C. The bacteria were harvested by centrifugation, suspended in lysis buffer (50 mM Hepes, pH 7.5, 150 mM NaCl, and protease inhibitors (Calbiochem), and sonicated. The cell debris were separated from the soluble fraction by centrifugation (18000g, 15 min). The soluble fraction was applied on a cobalt column (Talon, Qiagen). The column was washed with lysis buffer, and eluted with 2, 10 and 100 mM imidazole in the same buffer. The fractions containing highly purified recombinant proteins were pooled and dialyzed against 20 mM Hepes, pH 7.5, 150 mM NaCl.

2.3 In vitro *glucosylation*

Glucosylation of small GTPases was achieved as followed according to (Popoff *et al.*, 1996). 2 μl of UDP-[^{14}C]Glucose or UDP-[^{14}C]-*N*-acetylglucosamine in ethanol (O.2 μCi, 300 mCi/mmol; DuPont NEN, les Ulis France) was dried under vacuum; 1 μg of GST-GTPase protein in a final volume of 20 μl of glucosylation buffer (50 mM triethanolamine pH 7.5, 2 mM $MgCl_2$, 0.3 mM GDP) were added to the dried UDP-[^{14}C]Glucose. One μl of rN-TpeL (2 mg/ml) was added to start the reaction, which was carried out for 1 h at 37°C. The reaction was stopped by adding 5 μl of 2 x SDS sample buffer, boiled and electrophoresed on a 15% SDS-polyacrylamide gel. After staining with Coomassie blue, followed by distaining, the gel was dried and autoradiographed.

2.4 Peptide analysis by HPLC, sequencing and mass spectrometry

cH-Ras (5 μg) was incubated without or with rN-TpeL (10^{-7} M) in glucosylation buffer containing UDP-*N*-acetylglucosamine (5 mM) for 3 h at 37°C. Ras was the subjected to SDS-(14%)PAGE and stained with Amido Black. Ras bands were cut from the gel, washed with distilled water, dried, and resuspended in 150 μl of 50 mM Tris-HCl (pH 8.6) containing 0.001% Tween 20 and 0.2 μg of trypsin (Promega). Following18 h at 30°C, the preparations were centrifuged, the pellets were washed with 100 μl of 50 mM Tris-HCl (pH 8.6) containing 0.05% SDS and then with 100 μl 60% acetonitrile. The supernatants were recovered and concentrated to 100 μl by Speed Vac. Samples were injected onto a DEAE-HPLC column (Interchim Hema Bio 1000 DEAE, 33 x 1 mm) linked to a C18 reverse phase

HPLC column (Interchim Uptisphere ODBD, 150 x 1 mm) eluted with 2-70% acetonitrile gradient in 0.1% trifluoroacetic acid and monitored at 214 nm.

Separated peptides (1-2 µl on a ProteinChip gold array) were identified by their mass using SELDI-TOF-MS (PCS4000) from Bio-Rad (focus mass = 4000 daltons; laser intensity = 1100 nl). The matrix was α-cyano-4-hydoxycinnamic acid saturated in 50% acetonitrile, 0.5% trifluoroacetic acid.

2.5 MS and MS/MS analysis

Purified HPLC fractions were diluted in 10 µl of CHCA matrix (5 mg/ml in 70% ACN / 30 % H_2O / 0.1 % TFA) and 0.5 µl of them were spotted on the MALDI plate.

MS spectra were acquired in reflector positive mode using the 4800 MALDI TOF/TOF Analyzer (Applied Biosystems, USA) within a mass range of 800 to 4000 m/z. MS calibration was first carried out to a final mass accuracy of 1 ppm with a mixture of 5 standard peptides: des-Arg1 Bradykinin, $[M+H]^+$=904.468; Angiotensin, $[M+H]^+$=1296.685; Glu1-Fibrinopeptide, $[M+H]^+$=1570.677; ACTH 1-17, $[M+H]^+$=2093.087; ACTH 18-39, $[M+H]^+$=2465.199. MS spectra of the purified fractions were then acquired (3000 laser shots were averaged) and calibrated using the external default calibration (10 ppm mass accuracy).

MS/MS were performed in CID positive ion mode with a 2 kV collision energy of and air as collision gas. MS/MS calibration was performed using 4 CID fragments of the Glu1-Fibrinopeptide ($[M+H]^+$= 175.119, 684.346, 1056.475 and 1441.634) (mass accuracy of 10 ppm). 4000 to 10 000 laser shots were averaged to acquired MS/MS spectra of the selected precursors. Each spectrum was then calibrated using the external default calibration (mass accuracy of 100 ppm).

MS/MS queries were performed using the MASCOT search engine 2.1 (Matrix Science Ltd., UK) and the SwissProt 57.4 database (470369 sequences; 166709888 residues) with the following parameters: 50 ppm mass tolerance for the precursor and 0.3 Da for MS/MS fragments, trypsin cleavage. Hexose-*N*-acetylglucosamine (HexNAc) and oxidation of methionins were used as variable modifications. In these conditions, the minimal MASCOT score was 28 for a peptide confidence index ≥ 95%.

3. Results

3.1 TpeL is a glucosyltransferase which targets Ras proteins

As previously found (Amimoto et al., 2007), TpeL shows a significant overall sequence homology with the LCGTs and contains a conserved active enzymatic site (DxD) in the N-terminal part, except that the total protein length is shorter (190 kDa) than that of the glucosylating toxins from *C. difficile*, *C. sordellii* or *C. novyi* (250 to 300 kDa) (Jank and Aktories, 2008; Just and Gerhard, 2004; Popoff and Bouvet, 2009; Rupnik and Just, 2006). The N-terminal domain (amino acid 1 to 543) of LCGTs is the intracellular active domain, which is released into the cytosol through an autoproteolytic process during the toxin endocytosis (Jank and Aktories, 2008). Interestingly, the TpeL N-terminal domain shows a high level of sequence similarity with that of the other LCGTs with an intermediate position between the N-terminal domain of *C. novyi* alpha toxin and those of the *C. difficile* and *C. sordellii* glucosylating toxins (Fig. 1). Therefore, we produced and purified the N-terminal domain of TpeL as recombinant protein (Fig. 3) to check its enzymatic activity. In a first series of experiments we used Rho, Rac, Cdc42 and cH-Ras, which are the representative substrates of LGCTs, in a glucosylation assay with TpeL. As shown in Fig. 2B, TpeL N-terminus glucosylated only cH-Ras and no RhoA, Rac1 or Cdc42. In addition, the glucosylation of cH-Ras was more efficient by using UDP-*N*-acetylglucosamine than UDP-glucose as cosubstrate. Thereby, recombinant TpeL N-terminal part contains a glucosyltransferase activity specific of cH-Ras protein but not of Rho and Cdc42.

3.2 TpeL preferentially uses UDP-N-acetylglucosamine as cosubstrate

In order to determine the cosubstrate requirement for TpeL (10^{-7} M) activity, kinetics of cH-Ras glucosylation was performed in the presence of UDP-[^{14}C]-glucose or UDP-[^{14}C]-*N*-acetylglucosamine (Fig. 3 A). An almost complete glucosylation of cH-Ras was obtained with TpeL in the presence of UDP-[^{14}C]-*N*-acetylglucosamine, whereas the reaction with UDP-[^{14}C]-glucose had longer kinetics (Fig. 3A and B). The level of cH-Ras glucosylation was about 100 fold less with UDP-glucose compared to UDP-*N*-acetylglucosamine. Even after longer incubation period (until 2 h), a 100-fold difference in enzymatic level was observed between both cosubstrates (not shown).

Then, we investigated if UDP-*N*-acetylglucosamine was the only efficient cosubstrate of TpeL by a competition assay using cH-Ras, UDP-[^{14}C]-*N*-acetylglucosamine, and various non-radioactive hexose derivatives. As expected, non-radioactive UDP-*N*-acetylglucosamine totally blocked the transfer of [^{14}C]-*N*-acetylglucosamine from UDP-[^{14}C]-*N*-acetylglucosamine on cH-Ras, whereas *N*-acetylglucosamine was inefficient (Fig. 3C and D).

UDP-glucose and UDP-mannose, a close isoform of UDP-glucose, were also as efficient as UDP-*N*-acetylglucosamine to block the TpeL-dependent glucosylation of cH-Ras. The other UDP derivatives (UDP-galactose, UDP-glucuronic acid, and UDP-galacturonic acid) also inhibited the glucosylation of cH-Ras but to a lower extent. Among the other nucleoside-diphosphate hexose derivatives, GDP-glucose partially prevented cH-Ras glucosylation. TDP-glucose which contains a pyrimidine base as UDP, was not effective to compete the reaction. This suggests that UDP is a major structure which is recognized by TpeL.

3.3 Ras is the main substrate of TpeL

Next, we investigated the substrates of TpeL. Using a large set of recombinant small GTPases and UDP-*N*-acetylglucosamine as cosubstrate, we checked the TpeL activity in the *in vitro* glucosylation assay. As shown in Fig. 4A, Ras proteins including cH-Ras, K-Ras, and N-Ras were the main substrates which were efficiently glucosylated by TpeL. In addition, R-Ras3 and Rap1a, which also belong to the Ras family of proteins, were glucosylated by TpeL, but to a lower extent. The glucosylation level of R-Ras3 was 16% from that of Ras, and that of Rap1a 6% (Fig. 4B). No proteins from the Rho family nor Rab6 and Arf1, representative proteins from the Rab and Arf families, were substrates of TpeL, except Rac1 which was very weakly modified compared to cH-Ras (Fig. 4A). Thereby, TpeL contains a glucosyltransferase activity targeting Ras proteins, and predominantly cH-Ras, K-Ras, and N-Ras.

3.4 TpeL glucosylates cH-Ras at Thr35

In an effort to identify the cH-Ras residue or residues that are modified by TpeL, cH-Ras (5 µg) was incubated with TpeL (10^{-7} M), non-radioactive UDP-*N*-acetylglucosamine (10 mM) in glucosylation buffer during 3 h at 37°C and then analyzed by SELDI-TOF using a Q10 chip (strong anionic exchanger). cH-Ras prepared in the same conditions but without TpeL was used as reference. As shown in Fig. 5, cH-Ras treated with TpeL in the presence of UDP-*N*-acetylglucosamine has an increase in mass of 205, which correlates with an addition of a one HexNAc molecule (MW 203). This indicates that TpeL catalyzes the transfer of one HexNAc molecule per cH-Ras molecule.

Next, cH-Ras treated with rN-TpeL or untreated was run on a SDS-PAGE, trypsin digested, and the resulting peptides were separated by HPLC. As shown in Fig. 6A, fraction 14 from rN-Tpel-treated cH-Ras has an increased retention time which corresponds to an increased mass of 203 daltons compared to fraction 15 of untreated cH-Ras as determined by

SELDI-TOF (Fig. 6B). N-terminal sequencing of fractions14 and 15 showed that the peptides with the sequence SALT and SALTIQ, respectively. This indicates that fraction 14 from rN-TpeL treated cH-Ras and fraction 15 from untreated cH-Ras contained the same trypsin cleavage peptide SALTIQLIQNHFVDEYDPTIEDSYR. These results show that the residue modified by rN-TPEL and resulting from an addition of an HexNAc is part of the peptide SALTIQLIQNHFVDEYDPTIEDSYR which contains two Thr residues.

Fractions 14 and 15 were further analyzed by MS and MSMS followed by MASCOT searching (Fig. 7 and supplementary Fig. 1 and 2). HexNAc modification was identified on Thr19 of the peptide which corresponds to Thr35 of cH-Ras.

4. Discussion

It is reported that TpeL is produced by several *C. perfringens* types including types A, B and C and its gene localization on plasmid accounts for horizontal transfer between *C. perfringens* strains (Amimoto et al., 2007; Sayeed *et al.*, 2010). TpeL synthesis seems to be dependent of the sporulation (Paredes-Sabja *et al.*, 2011) and this novel toxin likely represents an additional virulence factor involved in necrotic enteritis in poultry (Coursodon *et al.*, 2012). Indeed, TpeL is cytotoxic to various cell lines by inducing apoptosis via impairment of the Ras signaling pathway (Guttenberg et al., 2012). However some *C. perfringens* strains, like MC18, seems to contain a truncated *tpel* gene resulting in a protein lacking 128 C-terminal amino acids which is not cytotoxic (Guttenberg et al., 2012). In our experience, only a few *C. perfringens* strains type C isolated from necrotic enteritis in piglets, and a *C. perfringens* type A strain isolated from food contain *tpel* gene.

TpeL is related to the LCGTs based on amino acid sequence identity and shows the highest similarity with TcnA. We have analyzed the enzymatic properties of TpeL, from which most of them have been published during the progress of this work (Guttenberg et al., 2012; Nagahama et al., 2011). Albeit confirmatory in a large part, our investigations bring complementary data. TpeL is a glucosytransferase, which retains the enzymatic site DxD of LCGTs and with a global amino acid sequence identity more related to TcnA than to the other LCGTs (Fig. 1). In addition, TpeL displays the same motif, $A_{383}NQ_{385}$, of co-substrate specificity than TcnA, which uses UDP-*N*-acetylglucosamine as sugar donor, instead of $I_{383}NQ_{385}$ in the other LCGTs which catalyzes the transfer of glucose from UDP-glucose (Guttenberg et al., 2012). Using the recombinant catalytic domain (1-543), we showed that TpeL exhibited both UDP-glucosylation and UDP-*N*-acetylglucosamination (GlcNAcylation) activities towards cH-Ras, but with a 100 fold more efficiency of GlcNAcylation. UDP is the

major binding determinant since the rN-TpeL GlcNAcylation was impaired by all UDP-hexoses tested in competition assay (Fig. 3C and D). However, UDP-glucose and UDP-*N*-acetylglucosamine were more efficient competitors than the other UDP-hexoses, indicating a stringent specificity for these two cosubstrates. In contrast, Nagahama et al. report a TpeL enzymatic competition only with UDP-glucose and UDP-*N*-acetylglucosamine and no with other UDP-hexoses (Nagahama et al., 2011). The bases of these discrepant results are not clear, in our study, the recombinant N-terminal TpeL 1-543 amino was used instead TpeL 1-525 by Nagahama et al. (Nagahama et al., 2011).

As previously found, the three isoforms of Ras including cH-Ras, N-Ras and K-Ras are the main substrates of Tpel. Using a large panel of small GTPases, we observed that rN-TpeL modified cH-Ras, N-Ras and K-Ras and to a lower extent Rap1a and R-Ras3. In contrast to previous findings [Guttenberg, 2012 #3074;Nagahama, 2011 #3076], we showed that Rac1 was a very poor substrate of TpeL in the presence of UDP-*N*-acetylglucosamine. Only a weak glucosamination was evidenced after a long exposure of the autoradiographies and no Rac glucosylation was observed with rN-TpeL and UDP-glucose. In agreement with Guttenberg et al. (Guttenberg et al., 2012) we showed no modification of Ral by TpeL in the presence of UDP-*N*-acetylglucosamine or UDP-glucose, whereas Ral has been reported to be a TpeL substrate by Nagahama and coworkers (Nagahama et al., 2011). These different observations might result from the distinct recombinant TpeL fragments used in each study. We confirmed by *in vitro* glucosylation and mass spectrometry thet TpeL modifies Ras at Thr35. In our conditions, TpeL displays glucosyltransferase activity only with Ras proteins, mainly the three isoforms of Ras and weakly Rap1a and R-Ras3, and is not active with Rho proteins. This opens the way to delineate specific tools directed towards Ras for therapeutic purpose and cell biology investigations.

Acknowledgement

This was supported by Institut Pasteur funding.

References

Amimoto, K., Noro, T., Oishi, E., Shimizu, M., 2007. A novel toxin homologous to large clostridial cytotoxins found in culture supernatant of Clostridium perfringens type C. Microbiology 153, 1198-1206.

Coursodon, C.F., Glock, R.D., Moore, K.L., Cooper, K.K., Songer, J.G., 2012. TpeL-producing strains of Clostridium perfringens type A are highly virulent for broiler chicks. Anaerobe 18, 117-121.

Guttenberg, G., Hornei, S., Jank, T., Schwan, C., Lu, W., Einsle, O., Papatheodorou, P., Aktories, K., 2012. Molecular characteristics of Clostridium perfringens TpeL toxin and consequences of mono-O-GlcNAcylation of Ras in living cells. J Biol Chem 287, 24929-24940.

Hofmann, F., Busch, C., Aktories, K., 1998. Chimeric clostridial cytotoxins: identification of the N-terminal region involved in protein substrate recognition. Infect. Immun. 66, 1076-1081.

Hofmann, F., Busch, C., Prepens, U., Just, I., Aktories, K., 1997. Localization of the glucosyltransferase activity of *Clostridium difficile* Toxin B to the N-terminal part of the holotoxin. J. Biol. Chem. 272, 11074-11078.

Jank, T., Aktories, K., 2008. Structure and mode of action of clostridial glucosylating toxins: the ABCD model. Trends Microbiol 16, 222-229.

Jank, T., Giesemann, T., Aktories, K., 2007. Clostridium difficile glucosyltransferase toxin B-essential amino acids for substrate binding. J Biol Chem 282, 35222-35231.

Just, I., Gerhard, R., 2004. Large clostridial cytotoxins. Rev. Physiol. Biochem. Pharmacol. 152, 23-47.

Nagahama, M., Ohkubo, A., Oda, M., Kobayashi, K., Amimoto, K., Miyamoto, K., Sakurai, J., 2011. Clostridium perfringens TpeL glycosylates the Rac and Ras subfamily proteins. Infect Immun 79, 905-910.

Paredes-Sabja, D., Sarker, N., Sarker, M.R., 2011. Clostridium perfringens tpeL is expressed during sporulation. Microb Pathog 51, 384-388.

Petit, L., Gibert, M., Popoff, M.R., 1999. *Clostridium perfringens*: toxinotype and genotype. Trends Microbiol. 7, 104-110.

Popoff, M.R., Bouvet, P., 2009. Clostridial toxins. Future Microbiol 4, 1021-1064.

Popoff, M.R., Chaves-Olarte, E., Lemichez, E., Von Eichel-Streiber, C., Thelestam, M., Chardin, P., Cussac, D., Antonny, B., Chavrier, P., Flatau, G., Giry, M., de Gunzburg,

J., Boquet, P., 1996. Ras, Rap, and rac small GTP-binding proteins are targets for *Clostridium sordellii* lethal toxin glucosylation. J. Biol. Chem. 271, 10217-10224.

Reinert, D.J., Jank, T., Aktories, K., Schulz, G.E., 2005. Structural basis for the function of Clostridium difficile toxin B. J Mol Biol 351, 973-981.

Rupnik, M., Just, I., 2006. Large clostridial cytotoxins modifying small GTPases, in: Alouf, J.E., Popoff, M.R. (Eds.), The Sourcebook of Bacterial Protein Toxins, 3° ed. Elsevier, Academic Press, Amsterdam, pp. 409-429.

Rupnik, M., Pabst, S., Rupnik, M., von Eichel-Streiber, C., Urlaub, H., Soling, H.D., 2005. Characterization of the cleavage site and function of resulting cleavage fragments after limited proteolysis of Clostridium difficile toxin B (TcdB) by host cells. Microbiology 151, 199-208.

Sayeed, S., Li, J., McClane, B.A., 2010. Characterization of virulence plasmid diversity among Clostridium perfringens type B isolates. Infect Immun 78, 495-504.

Ziegler, M.O., Jank, T., Aktories, K., Schulz, G.E., 2008. Conformational changes and reaction of clostridial glycosylating toxins. J Mol Biol 377, 1346-1356.

Figure legends

Figure 1. Phylogenetic tree of the whole toxin sequence (A) and enzymatic domain (543 N-terminal amino acids) (B) of TpeL (AB262081), TcdA (YP_001087137), TcdB (CAJ67492), TcdBF (CAC19891), TcsL6018 (X82638) and TcnA (CAA88565.1) according to the UP-GMA method. The percentage of replicate trees in which the associated taxa clustered together in the bootstrap test (100 replicates) are shown next to the branches. The tree is drawn to scale, with branch lengths in the same units as those of the evolutionary distances used to infer the phylogenetic tree. The evolutionary distances were computed using the Poisson correction method and are in the units of the number of amino acid substitutions per site.

Figure 2. TpeL N-terminal part glucosylates Ras but not Rho, Rac, and Cdc42. (A) SDS-PAGE of recombinant N-terminal part of TpeL stained with Blue Coomassie R-250. (B) Glucosylation of Ras, Rho, Rac, or Cdc42 (1 μg recombinant protein) by TpeL N-terminal part (10^{-7} M) in the presence of UDP-[^{14}C]Glucose or UDP-[^{14}C]-*N*-acetylglucosamine for 1 h at 37°C. The proteins were run on a SDS-PAGE and autoradiographed.

Figure 3. TpeL uses preferentially UDP-*N*-acetylglucosamine as cosubstrate. A kinetics of Ras glucosylation by rN-TpeL. Ras (1 μg) was incubated with rN-TpeL (10^{-7} M) for 1, 5, 10, 15 or 30 min at 37°C in glucosylation buffer containing 7 μM UDP-[^{14}C]-*N*-acetylglucosamine or UDP-[^{14}C]-glucose. The samples were electrophoresed on a SDS-(14%)PAGE, autoradiographed, and band intensity was quantified by ImageJ (NIH, USA). Experiments were done in triplicate. Means +/_ standard deviation are shown. (B) Kinetics of Ras glucosylation by rN-TpeL with UDP-[^{14}C]-glucose as in A but with a different scale of Y axis. Note that Ras glucosylation with UDP-[^{14}C]-glucose is about 100 fold less than with UDP-[^{14}C]-*N*-acetylglucosamine. (C) Competition assay of Ras glucosylation with various hexose derivatives. Ras (1 μg) was incubated in glucosylation buffer with rN-Tpel (10^{-7} M) and each of the various hexose derivatives (5 mM) for 30 min at 37°C. Then UDP-[^{14}C]-*N*-acetylglucosamine was added and the preparations were incubated at 37°C for additional 30 min and processed as described above. (D) Quantification of the competition assays.

Figure 4. TpeL recognizes specifically Ras. (A) Glucosylation of recombinant small GPTases (1 μg) with rN-Tpel (10^{-7} M) and UDP-[^{14}C]-*N*-acetylglucosamine was performed as described in Experimental Procedures for 1 h at 37°C. (B) Quantification of the glucosylated small GTPases. Glucosylation of Ras was defined as 100%.

Figure 5. Mono-*N*-acetylglucosaminylation of cH-Ras by TpeL. cH-Ras untreated and treated by rN-TpeL (10^{-7} M) in glucosylation buffer containing 5 mM UDP-*N*-acetylglucosamine for 3 h at 37°C was analyzed by SELDI-TOF mass spectrometry with a Q10 array. Ras treated with rN-TpeL shows an increased mass of 205 Da.

Figure 6. Identification of Ras peptide containing the TpeL modification. (A) Ras untreated and treated by rN-TpeL (10^{-7} M) in glucosylation buffer containing 5 mM UDP-*N*-acetylglucosamine for 3 h at 37°C was trypsin digested and analyzed by HPLC on a DEAE column linked to a C18 reverse phase column. Fraction 15 from untreated Ras and fraction 14 from rN-TpeL treated Ras were found to contain the same peptide SALTIQLIQNHFVDEYDPTIEDSYR by N-terminal sequencing,. (B) SELDI-TOF mass spectrometry showing that the peptide from fraction 14 (rN-TpeL-treated Ras) has an increased mass of 203 Da versus that of the parental peptide (fraction 15) from untreated Ras.

Figure 7. TpeL mono-*N*-acetylglucosaminates Ras at Thr35. MS and MS-MS spectrum of fraction 14 from rN-TpeL-treated Ras (A) and fraction 15 from untreated Ras (B).

Supplementary Figure 1. Mascot search results of MS-MS residues of peptide from fraction 14 (rN-TpeL-treated Ras).

Supplementary Figure 2. Mascot search results of MS-MS residues of peptide from fraction 15 (untreated Ras).

Conflict of Interest Statement

Click here to download high resolution image

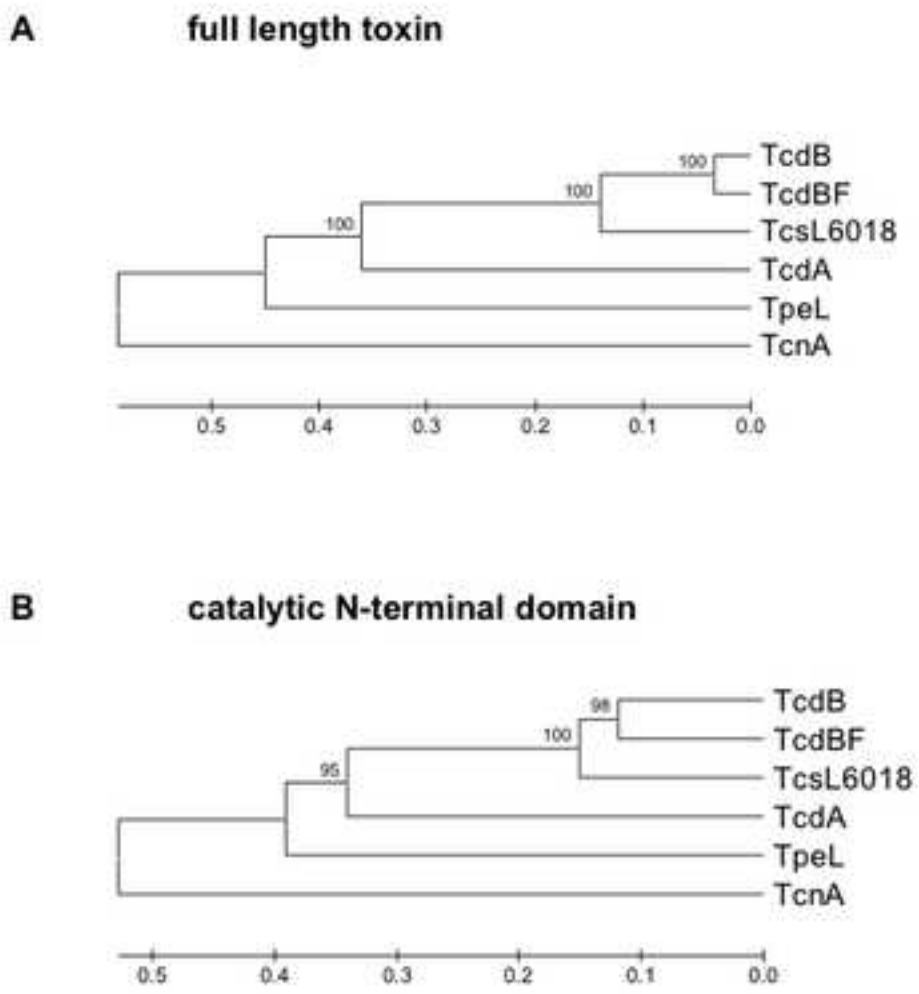

Figure 1

Figure
Click here to download high resolution image

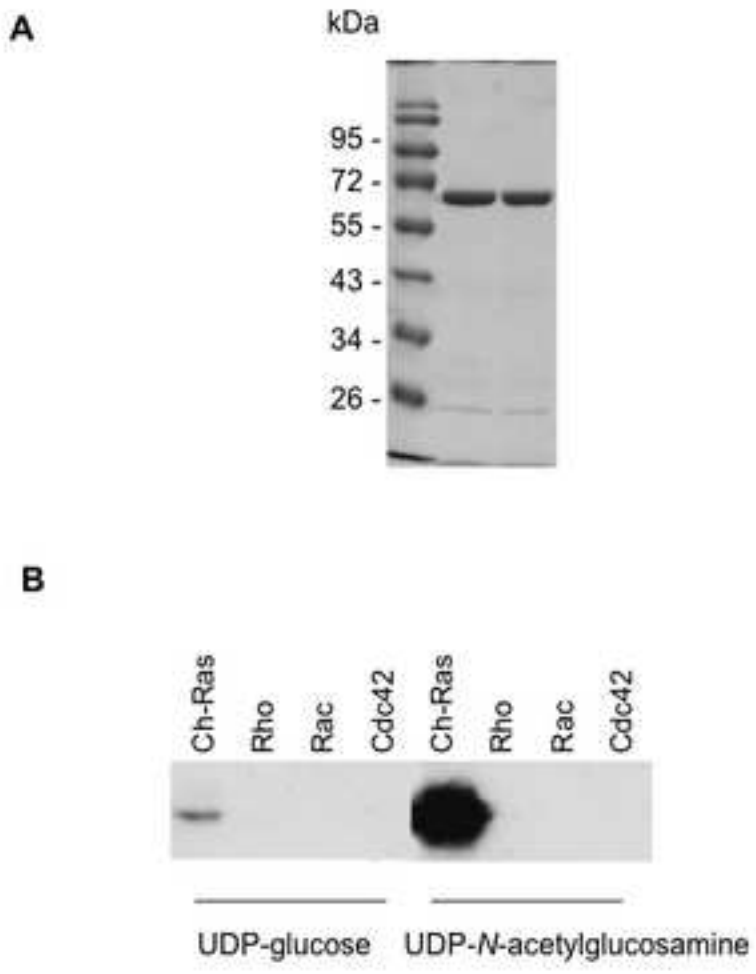

Figure 2

Figure
Click here to download high resolution image

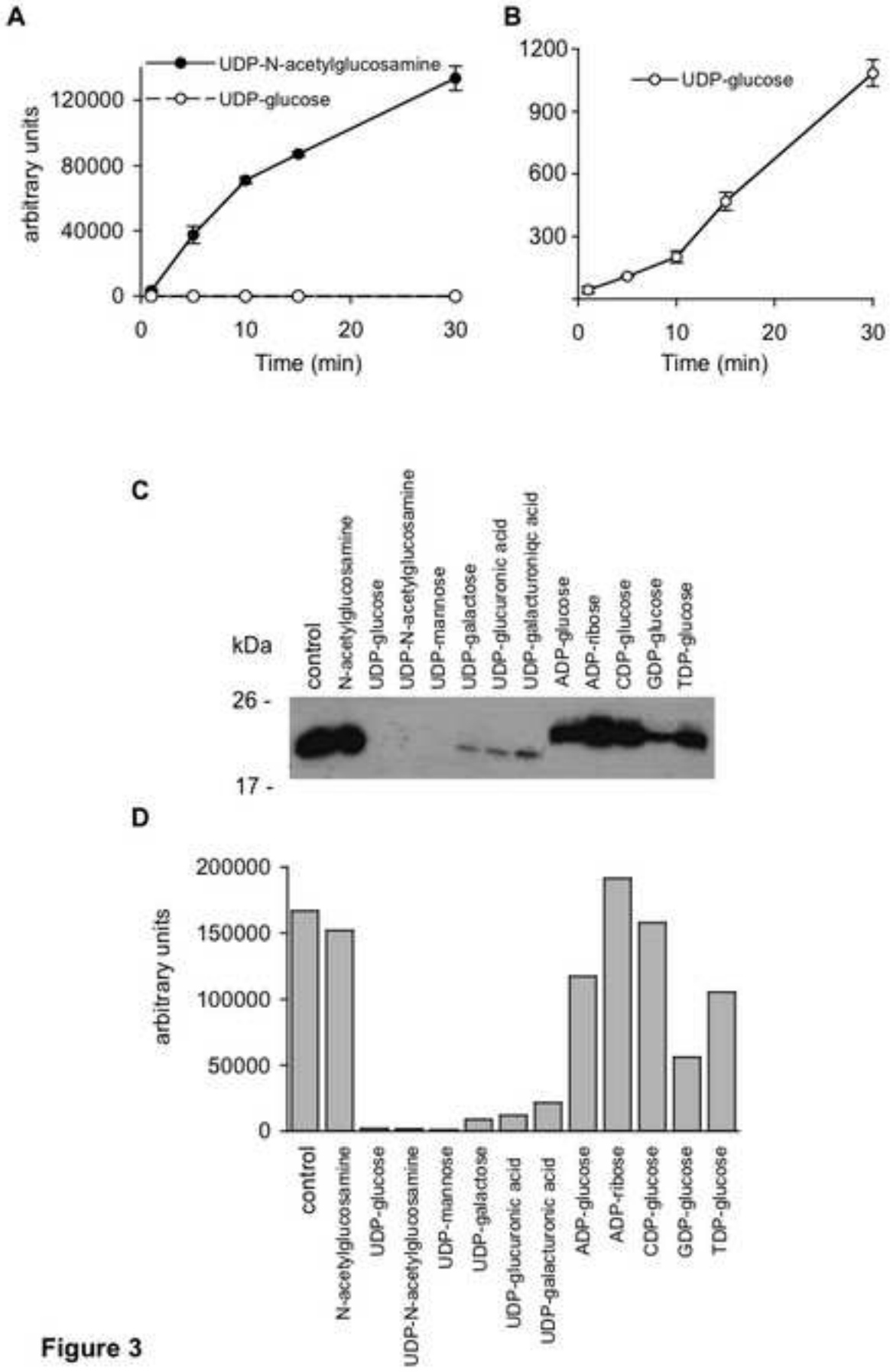

Figure 3

Figure
Click here to download high resolution image

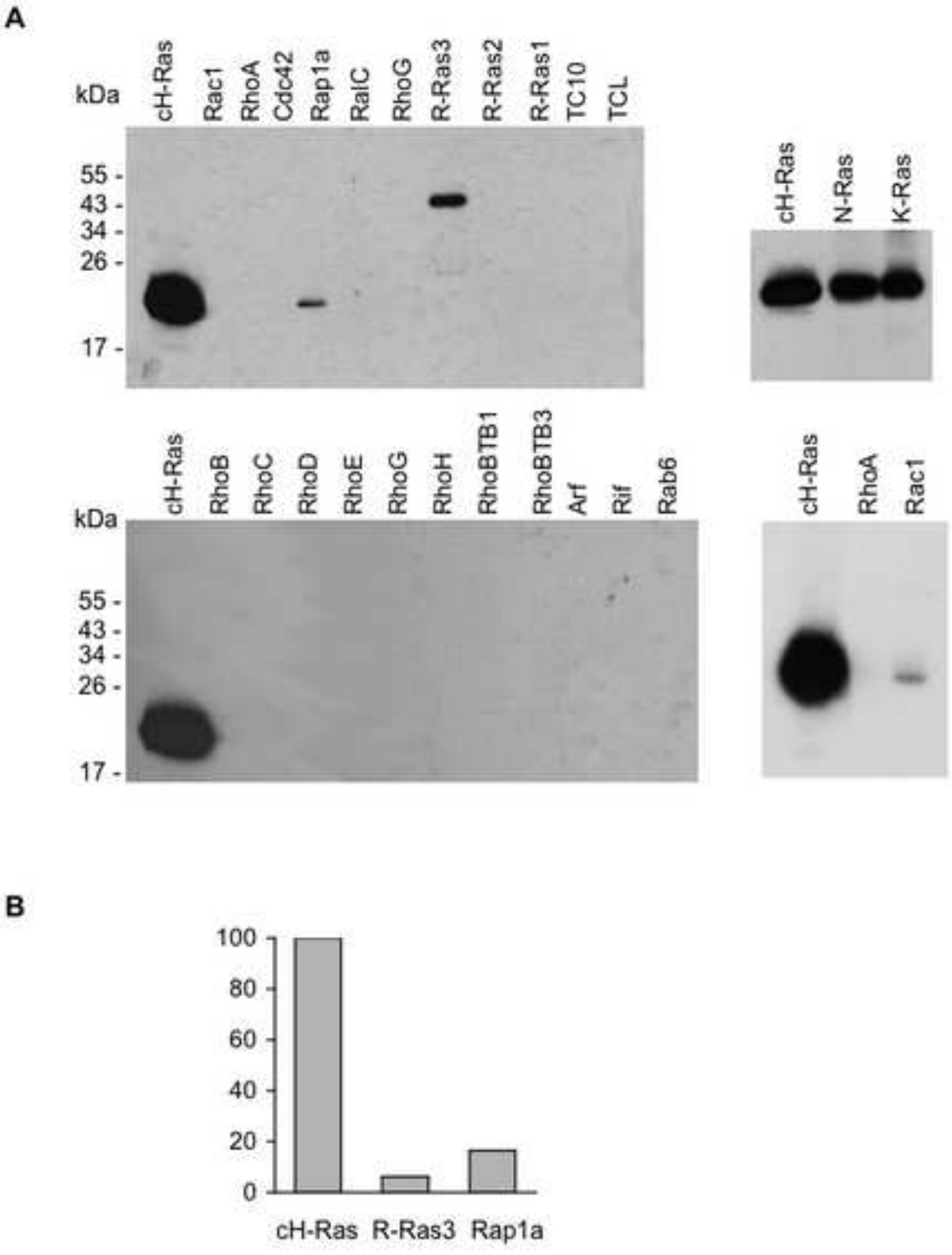

Figure 4

Figure

Click here to download high resolution image

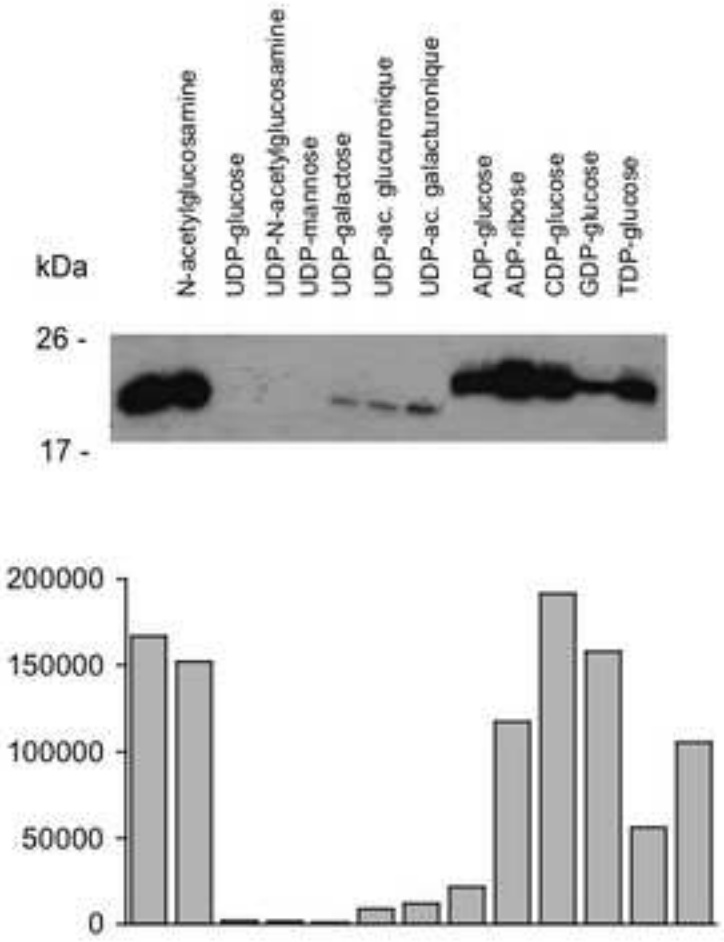

Figure
Click here to download high resolution image

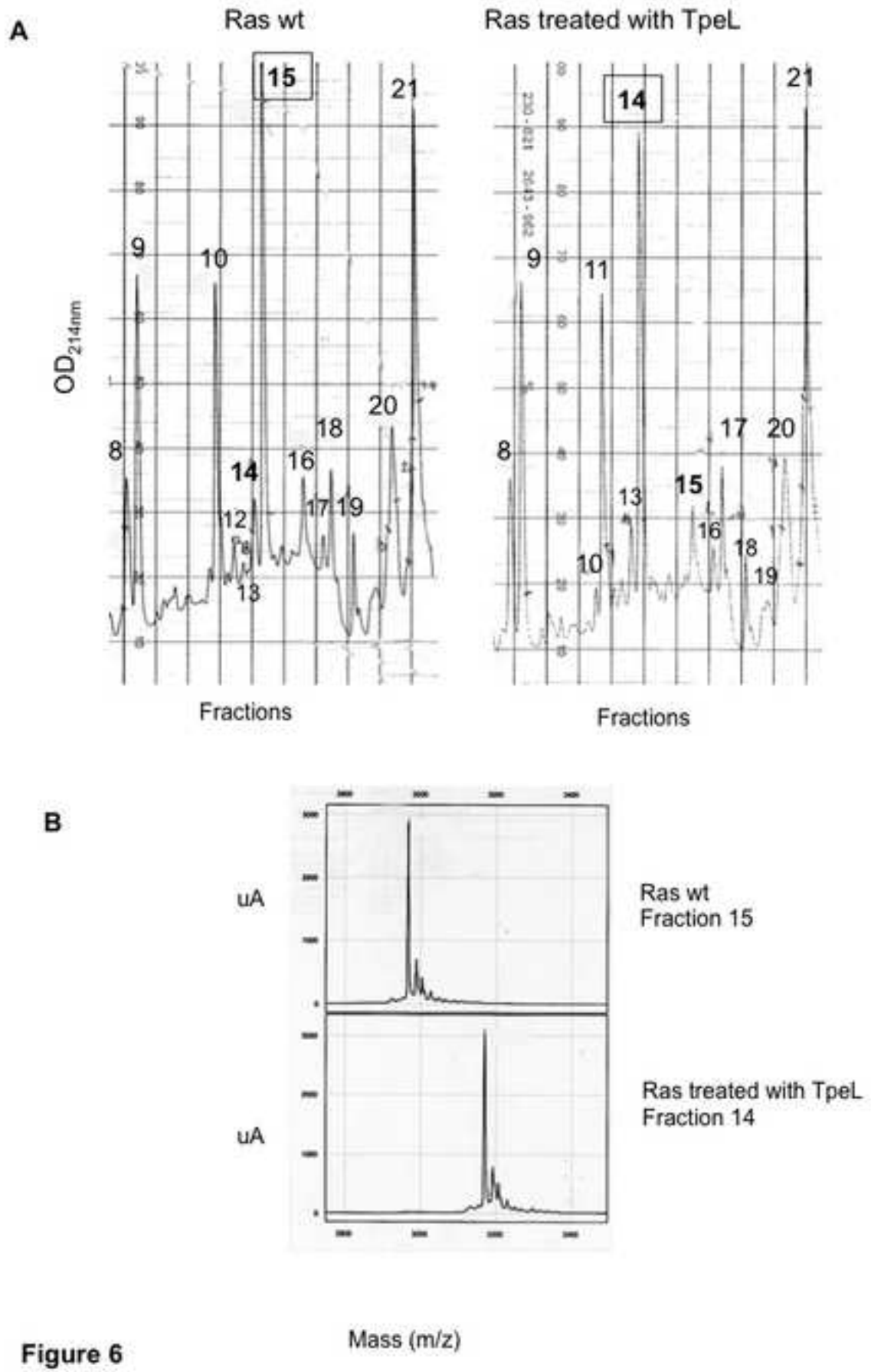

Figure 6

Figure
Click here to download high resolution image

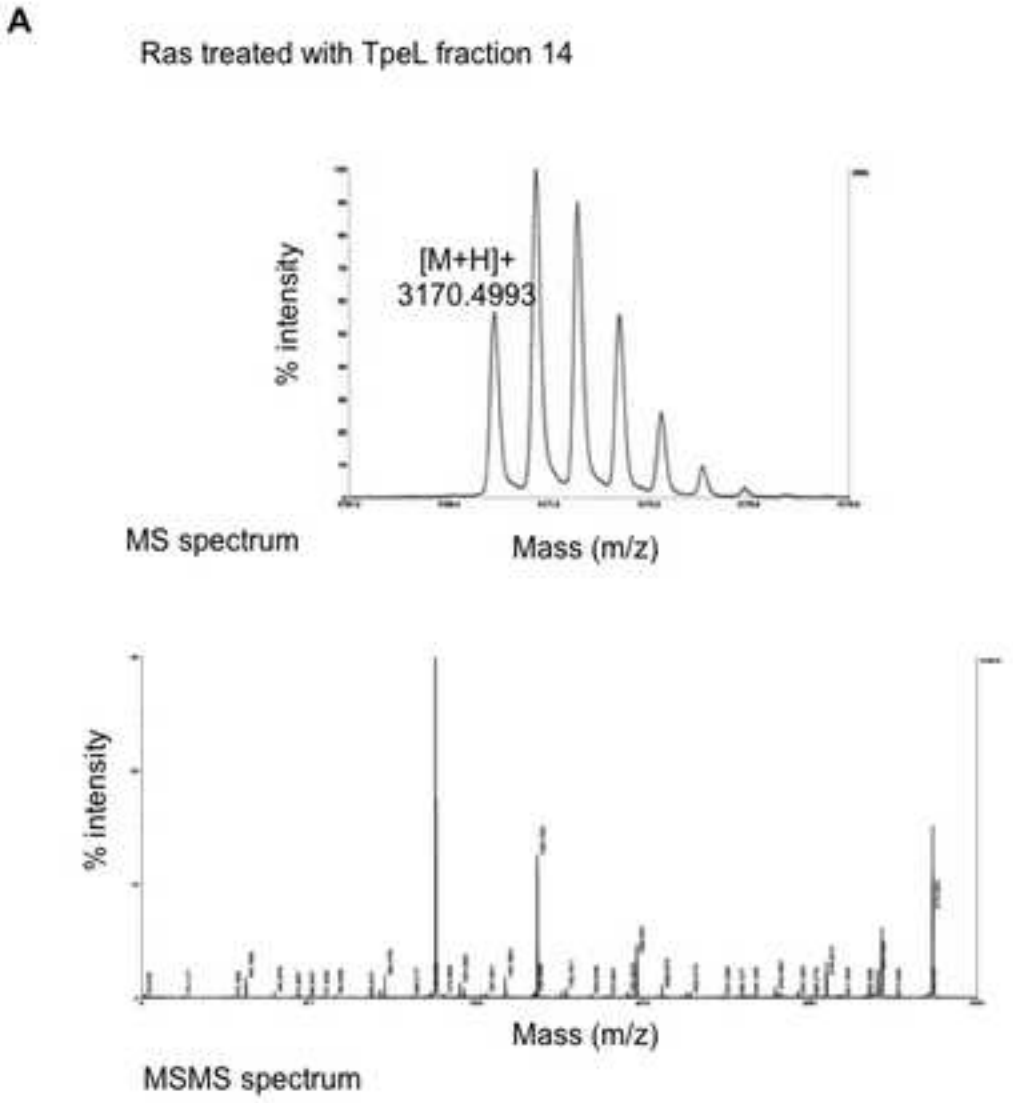

Figure 7

Figure
Click here to download high resolution image

B

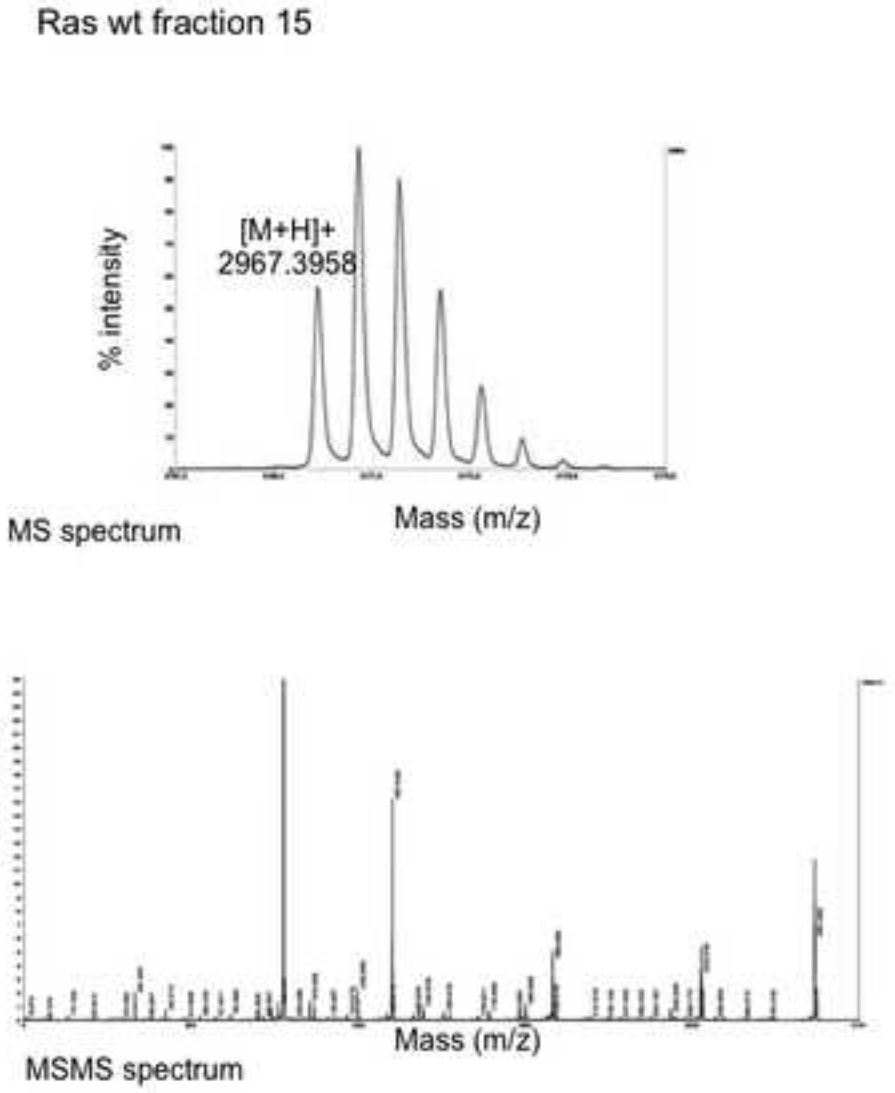

Figure 7 (followed)

Figure
Click here to download high resolution image

Ras treated with TpeL fraction 14

Mascot Search Results
Peptide View
MS/MS Fragmentation of **SALTIQLIQNHFVDEYDPTIEDSYR**
Found in **RASH_HUMAN**, GTPase HRas OS=Homo sapiens GN=HRAS PE=1 SV=1
Match to Query 1: 3169.491724 from(3170.499000,1+)

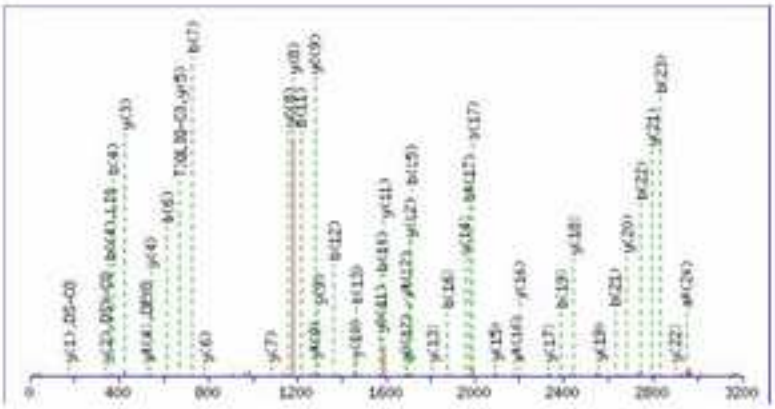

Monoisotopic mass of neutral peptide Mr(calc): 3169.5091
Variable modifications:
T19 : HexNAc (T)
Ions Score: 160 **Expect:** 3.3e-015
Matches (grey background): 54/439 fragment ions using 85 most intense peaks

#	Immon.	a	a*	a°	b	b*	b°	Seq	y	y*	y°	#
1	60.0444	60.0444		42.0338	88.0393		70.0287	S				25
2	44.0495	131.0815		113.0709	159.0764		141.0659	A	3067.4531			24
3	86.0964	244.1656		226.1550	272.1605		254.1499	L	2954.3690	2953.3738		23
4	74.0600	345.2132		327.2027	373.2082		355.1976	T	2853.3213	2866.3417	2868.3210	22
5	86.0964	458.2973		440.2867	486.2922		468.2817	I	2740.2373	2753.2577	2767.2733	21
6	101.0709	586.3559	569.3293	568.3453	614.3508	597.3242	596.3402	Q	2612.1787	2611.1834		20
7	86.0964	699.4399	682.4134	681.4294	727.4349	710.4083	709.4243	L	2499.0946	2498.0994		19
8	86.0964	812.5240	795.4975	794.5134	840.5189	823.4924	822.5084	I	2386.0106	2399.0310	2413.0466	18
9	101.0709	940.5826	923.5560	922.5720	968.5775	951.5509	950.5669	Q	2257.9520	2256.9567		17
10	87.0553	1054.6255	1037.5990	1036.6149	1082.6204	1065.5939	1064.6099	N	2143.9091	2142.9138		16
11	110.0713	1191.6844	1174.6579	1173.6739	1219.6793	1202.6528	1201.6688	H	2006.8502			15
12	120.0808	1338.7528	1321.7263	1320.7423	1366.7477	1349.7212	1348.7372	F	1859.7817			14
13	72.0808	1437.8212	1420.7947	1419.8107	1465.8162	1448.7896	1447.8056	V	1760.7133	1773.7337		13
14	88.0393	1552.8482	1535.8216	1534.8376	1580.8431	1563.8165	1562.8325	D	1645.6864	1644.6911		12
15	102.0550	1681.8908	1664.8642	1663.8802	1709.8857	1692.8591	1691.8751	E	1516.6438	1515.6486		11
16	136.0757	1844.9541	1827.9276	1826.9435	1872.9490	1855.9225	1854.9385	Y	1353.5805			10
17	88.0393	1959.9810	1942.9545	1941.9705	1987.9760	1970.9494	1969.9654	D	1238.5535	1237.5583		9
18	70.0651	2057.0338	2040.0073	2039.0232	2085.0287	2068.0022	2067.0182	P	1141.5008	1140.5055		8
19	277.1394	2361.1609	2344.1343	2343.1503	2389.1558	2372.1292	2371.1452	T	837.3737	850.3941	852.3734	7
20	86.0964	2474.2449	2457.2184	2456.2344	2502.2398	2485.2133	2484.2293	I	724.2897	737.3101	751.3257	6
21	102.0550	2603.2875	2586.2610	2585.2769	2631.2824	2614.2559	2613.2719	E	595.2471	594.2518		5
22	88.0393	2718.3144	2701.2879	2700.3039	2746.3094	2729.2828	2728.2988	D	480.2201	479.2249		4
23	60.0444	2805.3465	2788.3199	2787.3359	2833.3414	2816.3148	2815.3308	S	393.1881	392.1928		3
24	136.0757	2968.4098	2951.3833	2950.3992	2996.4047	2979.3782	2978.3942	Y	250.1548			2
25	129.1135							R	74.0237	73.0284		1

Supplementary Figure 1

Figure
Click here to download high resolution image

RasH wt fraction 15

Mascot Search Results
Peptide View
MS/MS Fragmentation of **SALTIQLIQNHFVDEYDPTIEDSYR**
Found in **RASH_HUMAN**, GTPase HRas OS=Homo sapiens GN=HRAS PE=1 SV=1
Match to Query 1: 2966.388724 from(2967.396000,1+)

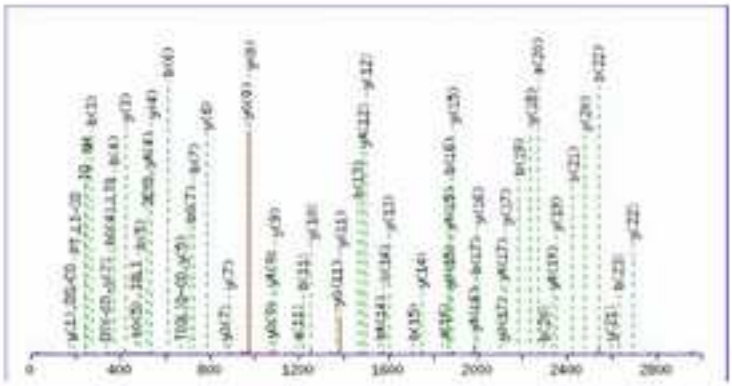

Monoisotopic mass of neutral peptide Mr(calc): 2966.4297
Ions Score: 191 **Expect:** 2.9e-018
Matches (grey background): 72/457 fragment ions using 83 most intense peaks

#	Immon.	a	a*	a°	b	b*	b°	Seq.	c	w	w'	y	y*	y°	#
1	60.0444	60.0444		42.0338	88.0393		70.0287	S							25
2	44.0495	131.0815		113.0709	159.0764		141.0659	A	2864.3737			2880.4093	2863.3784	2862.3944	24
3	86.0964	244.1656		226.1550	272.1605		254.1499	L	2751.2896	2750.2944		2809.3679	2792.3413	2791.3573	23
4	74.0600	345.2132		327.2027	373.2082		355.1976	T	2650.2420	2663.2624	2665.2416	2696.2630	2679.2573	2678.2733	22
5	86.0964	458.2973		440.2867	486.2922		468.2817	I	2537.1579	2550.1783	2564.1939	2595.2361	2578.2096	2577.2256	21
6	101.0709	586.3559	569.3293	568.3453	614.3508	597.3242	596.3402	Q	2409.0995	2408.1041		2482.3321	2465.1255	2464.1415	20
7	86.0964	699.4399	682.4134	681.4294	727.4349	710.4083	709.4243	L	2296.0153	2295.0200		2354.0933	2337.0670	2336.0829	19
8	86.0964	812.5240	795.4975	794.5134	840.5189	823.4924	822.5084	I	2182.9312	2195.9516	2209.9672	2241.0094	2223.9829	2222.9989	18
9	101.0709	940.5826	923.5560	922.5720	968.5775	951.5509	950.5669	Q	2054.8726	2053.8774		2127.9214	2110.8950	2109.9110	17
10	87.0553	1054.6255	1037.5990	1036.6149	1082.6204	1065.5939	1064.6099	N	1940.8297	1939.8344		1999.8660	1982.8303	1981.8562	16
11	110.0713	1191.6944	1174.6679	1173.6739	1219.6793	1202.6528	1201.6688	H	1803.7708			1869.8239	1866.7973	1867.8133	15
12	120.0808	1338.7528	1321.7263	1320.7423	1366.7477	1349.7212	1348.7372	F	1656.7024			1749.7650	1731.7384	1730.7544	14
13	72.0808	1437.8212	1420.7947	1419.8107	1465.8162	1448.7896	1447.8056	V	1557.6340	1570.6544		1601.6966	1584.6700	1583.6860	13
14	88.0393	1552.8482	1535.8216	1534.8376	1580.8431	1563.8165	1562.8325	D	1442.6070	1441.6118		1502.6293	1485.6028	1484.6176	12
15	102.0550	1681.8908	1664.8642	1663.8802	1709.8857	1692.8591	1691.8751	E	1313.5644	1312.5692		1387.6012	1370.5747	1369.5906	11
16	136.0757	1844.9543	1827.9276	1826.9435	1872.9490	1855.9225	1854.9385	Y	1150.5011			1259.5596	1241.5321	1240.5480	10
17	88.0393	1959.9810	1942.9545	1941.9705	1987.9760	1970.9494	1969.9654	D	1035.4742	1034.4789		1095.4965	1078.4697	1077.4857	9
18	70.0651	2057.0338	2040.0073	2039.0232	2085.0287	2068.0022	2067.0182	P	938.4214	937.4261		998.4643	981.4378	980.4538	8
19	74.0600	2158.0815	2141.0549	2140.0709	2186.0764	2169.0498	2168.0658	T	837.3737	850.3941	852.3734	903.4156	886.3890	885.4050	7
20	86.0964	2271.1655	2254.1390	2253.1550	2299.1605	2282.1339	2281.1499	I	724.2897	737.3101	751.3257	782.3679	765.3414	764.3573	6
21	102.0550	2400.2081	2383.1816	2382.1976	2428.2030	2411.1765	2410.1925	E	595.2471	594.2518		669.2839	652.2573	651.2733	5
22	88.0393	2515.2351	2498.2085	2497.2245	2543.2300	2526.2034	2525.2194	D	480.2201	479.2249		540.2631	523.2367	522.2527	4
23	60.0444	2602.2671	2585.2406	2584.2565	2630.2620	2613.2355	2612.2515	S	393.1881	392.1928		425.2141	408.1878	407.2037	3
24	136.0757	2765.3304	2748.3039	2747.3199	2793.3253	2776.2988	2775.3148	Y	230.1248			339.1832	321.1567		2
25	129.1135							R	74.0237	73.0284		175.1190	158.0924		1

Supplementary figure 2